American Journal of Pathology, Vol. 164, No. 6, June 2004

Acetylcholinesterase-Aβ Complexes Are More Toxic than Aβ Fibrils in Rat Hippocampus

Effect on Rat β-Amyloid Aggregation, Laminin Expression, Reactive Astrocytosis, and Neuronal Cell Loss

Ariel E. Reyes, Marcelo A. Chacón, Margarita C. Dinamarca, Waldo Cerpa, Carlos Morgan, and Nibaldo C. Inestrosa

From the Centro de Regulación Celular y Patología "Joaquín V. Luco," Millennium Institute of Fundamental and Applied Biology, Facultad de Ciencias Biológicas, Pontificia Universidad Católica de Chile, Santiago, Chile

Neuropathological changes generated by human amyloid-β peptide (Aβ) fibrils and Aβ-acetylcholinesterase (Aβ-AChE) complexes were compared in rat hippocampus *in vivo*. Results showed that Aβ-AChE complexes trigger a more dramatic response *in situ* than Aβ fibrils alone as characterized by the following features observed 8 weeks after treatment: 1) amyloid deposits were larger than those produced in the absence of AChE. In fact, AChE strongly stimulates rat Aβ aggregation *in vitro* as shown by turbidity measurements, Congo Red binding, as well as electron microscopy, suggesting that Aβ-AChE deposits observed *in vivo* probably recruited endogenous Aβ peptide; 2) the appearance of laminin expressing neurons surrounding Aβ-AChE deposits (such deposits are resistant to disaggregation by laminin *in vitro*); 3) an extensive astrocytosis revealed by both glial fibrillary acidic protein immunoreactivity and number counting of reactive hypertrophic astrocytes; and 4) a stronger neuronal cell loss in comparison with Aβ-injected animals. We conclude that the hippocampal injection of Aβ-AChE complexes results in the appearance of some features reminiscent of Alzheimer-like lesions in rat brain. Our studies are consistent with the notion that Aβ-AChE complexes are more toxic than Aβ fibrils and that AChE triggered some of the neurodegenerative changes observed in Alzheimer's disease brains. *(Am J Pathol 2004, 164:2163–2174)*

Alzheimer's disease (AD) is one of the most common neurodegenerative dementias, characterized by a progressive decline of cognitive functions and psychomotor abilities.[1] The hallmark neuropathological features of AD include localized neuronal cell death, extracellular senile plaques (SPs), and intracellular neurofibrillary tangles.[2,3] SPs are extracellular deposits of Aβ fibrils associated with dystrophic dendrites, reactive astrocytes, and activated microglia.[4] Amyloid is a heterogeneous structure with a nonuniform distribution in the brain, which contains a core of amyloid-β peptide (Aβ), a 40- to 42-amino acid peptide fragment derived from proteolytic processing of the amyloid precursor protein (APP).[3,5] Amyloid deposits are characterized histologically as consisting of fibrils, 4 to 10 nm in diameter, which exhibit a green fluorescent signal when stained with thioflavin-T (Th-T).[6] Histochemical and immunochemical methods also revealed numerous other proteins associated with amyloid plaque deposits. These proteins include apolipoprotein E,[7] α1-anti-chymotrypsin,[8] heparan sulfate proteoglycans,[9,10] laminin,[11] and acetylcholinesterase,[12,13] among others. Alterations in AChE expression and distribution have been reported in AD brains.[14–16] In fact, neuronal cell death in early stages of AD is related to the cholinergic system.[17] Transgenic overexpression of human AChE in mice induces a progressive cognitive deterioration suggesting that upsetting cholinergic balance may by itself cause progressive memory decline in mammals.[18–20] On the other hand, experiments in our laboratory have demonstrated that AChE promotes Aβ peptide fibrils assembly *in vitro*[21] and biochemical, physical, and morphological data strongly suggest that an amyloid-AChE complex is formed when AChE accelerates the assembly of Aβ peptides.[22] Such complexes were both Th-T fluorescence-positive and AChE activity-positive.[23] More important those complexes were more toxic for primary cultured chick retina neurons and PC12 cells than Aβ

Supported by the Centro de Regulación Celular y Patologia "Joaquín V. Luco"-Biomedicine (grant no. 13980001) and the Millennium Institute of Fundamental and Applied Biology (to N.C.I.).

Accepted for publication February 15, 2004.

Present address of A.E.R.: Facultad de Ciencias de la Salud, Universidad Diego Portales, Ejército 141, Santiago, Chile. Present address of C.M.: Laboratorio de Bioinformé, tica y expresión Génica, INTA, Universidad de Chile, Macul 5540, Santiago, Chile.

Address reprint requests to Dr. Nibaldo C. Inestrosa, Centro FONDAP-Biomedicina, P. Universidad Católica de Chile, Alameda 340, Santiago, Chile. E-mail: ninestr@genes.bio.puc.cl.

fibrils lacking AChE.[24] Interestingly, the toxicity of the Aβ-AChE complex was also dependent on the AChE concentration present in the complexes.[25,26] All these evidences are consistent with the possibility that local increments of AChE, as those present in AD brains,[12] should play a role in the neurodegeneration and cognitive deterioration observed in AD.[14,27] Our hypothesis implies that AChE plays a role in the pathological changes observed in AD by promoting amyloid formation and stability, astrocytosis, and neurotoxicity.

We decided, therefore, to evaluate and to compare *in vivo* the neurotoxicity of both Aβ fibrils and Aβ-AChE complexes. To perform these studies, we injected Aβ fibrils and Aβ-AChE complexes bilaterally in the rat dorsal hippocampus and the resulting neuropathological changes were studied. Results indicate that rats injected with Aβ-AChE complexes in the hippocampus form amyloid deposits that seem bigger in size than those observed in matched controls injected with the same amount of Aβ peptide, suggesting that endogenous rat Aβ may became incorporated into the amyloid deposits. The injection of Aβ-AChE complexes also results in the appearance of Alzheimer-like lesions in rat brain, and in all cases, the toxicity of the Aβ-AChE complex depends on the amount of enzyme present in the complexes.

Materials and Methods

Synthetic Peptides

Aβ peptide corresponding to residues 1 to 40 of the human wild-type sequence ($A\beta_{1\text{-}40}$) was obtained from Bachem (Torrance, CA) and the rat $A\beta_{1\text{-}40}$ peptide was obtained from Genemed Biotechnologies, Inc. (San Francisco, CA).

AChE Purification

Tetrameric G4 AChE form (sedimentation coefficient, 10.7 S) was purified from bovine caudate nucleus, using acridine affinity chromatography as previously described.[27] Both specific activity (6000 U/mg protein) and staining intensity after sodium dodecyl sulfate-polyacrylamide gel electrophoresis[28] were used to verify purity. AChE activity was determined by the method of Ellman and colleagues.[29]

Aβ Fibril Formation

Aβ fibrils were formed in a turbidity assay as previously described.[23,24] Briefly, Aβ peptide stock solution was prepared by dissolving freeze-dried aliquots of $A\beta_{1\text{-}40}$ in dimethyl sulfoxide (DMSO) at 15 mg/ml (3.5 mmol/L). An aliquot of this stock solution equivalent to 70 nmol of Aβ peptide was added to aqueous buffer (725 μl total volume; 0.1 mol/L Tris-HCl, pH 7.4). For the aggregation assay in the presence of AChE, an identical aliquot of the stock solution (70 nmol) was added to a buffer containing AChE (100 nmol/L) at a final molar ratio of AβμAChE = 1000:1. The solutions were stirred continuously (1350 rpm) at room temperature for 48 hours and then left at 4°C for another 48 hours. Aggregation was measured by turbidity at 400 nm against a buffer blank. Amyloid fibrils obtained were characterized by Congo Red (CR) binding.

CR-Binding Assay

Fibril aliquots were added to a solution containing 25 μmol/L CR solution, 100 mmol/L phosphate buffer (pH 7.4), and 150 mmol/L NaCl in a final volume of 960 μl, and incubated for 30 minutes at room temperature.[23] Absorbance was measured at 480 nm and 540 nm, and CR binding was determined by CR (concentration) = (A540/25,295) − (A480/46,306).[30]

β-Amyloid Disaggregation Assays

One hundred μmol/L of Aβ fibril suspensions were formed as described above either in the absence or the presence of 100 nmol/L AChE purified from bovine brain. Then, mouse laminin from Englebreth-Holm-Swarm tumor (Sigma L-2020 or Gibco catalog no. 23017-015; in 20 mmol/L Tris-HCl, 150 mmol/L NaCl, pH 7.2) was added to the fibril suspensions at a final laminin concentration as indicated in the legend of Figure 6. Th-T measurements were taken from 4-μl sample aliquots (added to 500 μl of 50 mmol/L phosphate buffer, pH 6.0, containing 15 μl of 0.1 mmol/L Th-T) at indicated incubation time points by monitoring fluorescence at λEx = 450 nm and λEm = 485 nm as described previously.[21,23]

Amyloid Fibril Purification

Assembled fibrils were washed four times with phosphate-buffered saline (PBS) at 14,000 rpm for 30 minutes to remove soluble peptide and AChE. Pellets were finally resuspended in artificial cerebrospinal fluid (ACF) at a concentration of 2.3 μg/μl Aβ peptide. Aliquots were mixed with a denaturing buffer and subjected to Tris-Tricine sodium dodecyl sulfate-polyacrylamide gel electrophoresis[31] to quantify Aβ peptide present into the fibrils by densitometry scanning. An Aβ peptide stock of known concentration was used as standard. Data was processed by a GS365W program from Hoeffer Scientific Instruments (San Francisco, CA). Before the injection treatment, we followed amyloid formation by turbidity at 400 nm and CR binding. Similar methods were used during Aβ fibril formation. The final products were analyzed using CR fibril staining under polarized light as well as by protease resistance assay (data not shown). All these assays did not show any apparent difference in the characteristic of the final amyloid product used for intracerebral injections.

Electron Microscopy of Amyloid Fibrils

The amyloid fibrils formed in turbidity assays were examined by electron microscopy. The fibrils were placed on Formvar carbon-coated 300-mesh nickel grids and neg-

atively stained with 1% phosphotungstic acid solution for 1 minute. Grids were examined under a Phillips EM-300 electron microscope at 60 kV.[21]

Surgical and Injection Protocol

Male Sprague-Dawley rats (280 to 320 g; 3 months old) were anesthetized with Equitesin (2.5 ml/kg), and injected bilaterally into the upper leaf of dentate gyrus in dorsal hippocampus (−3.5 mm anteroposterior, ±2.0 mm medial-lateral, −2.7 mm dorsal-ventral from the dura, according to bregma)[32] stereotaxically with a 10-μl Hamilton syringe with 27-gauge stainless steel needle. The injection is medial to granule layer and ventral to hippocampal fissure. The animals were injected bilaterally with 3 μl (at a rate of 0.5 μl/minute) of *in vitro* assembled Aβ fibrils formed in the presence ($n = 9$) or absence of AChE ($n = 9$), which is equivalent to 7 μg of Aβ peptide or Aβ-AChE complex into each hippocampus. Control animals were injected with an identical volume of ACF ($n = 6$). Two ($n = 3$) and eight ($n = 6$) weeks later, animals were fixed by intracardiac perfusion to perform histochemical procedures (see below).

Surgical and Infusion Protocol

Sprague-Dawley rats (280 to 320 g) were anesthetized with Equitesin (2.5 mg/kg, i.p.) and then rats were placed on a stereotaxic apparatus. These animals were with implanted a 27-gauge double cannula at the dorsal hippocampus under the coordinates mentioned above. Through a polyethylene hose, each cannula was connected to a 200-μl Alzet 2002 miniosmotic pump (Alza Corp., Mountain View, CA), which releases its content to a rate of 0.5 μl/hour. The pumps were placed under the skin back the head toward the rat shoulder. The pumps were charged with both soluble $A\beta_{1\text{-}40}$ peptide (0.75 μg/μl) and with AChE (0.272 μg/μl), final concentration in PBS to molar ratio of 1:200 (total volume, 200 μl). Fourteen days after this procedure, in the case of Figure 5, the procedure take 4 weeks, rats were fixed by perfusion with 4% paraformaldehyde and coronal brain sections were conducted for immunohistochemical analysis.

Perfusion and Fixation

Animals were anesthetized with Equitesin (2.5 ml/kg. i.p.) and injected with heparin (4 USP/kg, i.p.) to inhibit blood coagulation before perfusion. To study the evolution of amyloid deposits, rats were fixed at day 2 and 8 weeks after injection to visualize the evolution of amyloid deposits. Then they were perfused through the heart with perfusion buffer[33] containing 0.1% sodium nitrite, followed by fixation with 4% paraformaldehyde in 0.1 mol/L phosphate buffer (PB) for 30 minutes. Brains were removed from the skulls and postfixed in the same fixative for 3 hours at room temperature, followed by 10% sucrose in PB at 4°C overnight. After fixation, brains were coded to ensure unbiased processing and analysis. The brains were then cut into 50-μm coronal sections with a cryostat (Leitz 1900) at −20°C, from bregma −1.8 mm to bregma −4.8 mm.[32] Sections from the same brain were divided into six groups for analysis by the following procedures: Nissl staining (0.3% cresyl violet); immunohistochemical staining for glial fibrillary acidic protein (GFAP), laminin, and Aβ peptide; and CR and Th-S for specific amyloid staining.

Immunohistochemical Staining

Free-floating immunohistochemical procedure was performed as previously described.[34] Washing and dilution of immunoreagents was performed with 0.01 mol/L PBS with 0.2% Triton X-100 (PBS+T) throughout the experiments, and two PBS+T washes were performed after incubation with each antibody incubation. All three immunohistochemical procedures for each sample were performed simultaneously. Sections were pretreated with 0.3% H_2O_2 for 30 minutes to reduce endogenous peroxidase activity followed by treatment with 5% normal goat serum (DAKO, Carpinteria, CA) at room temperature for 1 hour to avoid nonspecific binding. GFAP, laminin, and Aβ detection was performed using the following antibodies: rabbit anti-GFAP polyclonal antibody (1:500) (DAKO), rabbit anti-laminin (1:60), and rabbit anti-$A\beta_{1\text{-}40}$ (1:100) (Sigma Chemical Co., St. Louis, MO) incubated overnight at 4°C. A horseradish peroxidase-conjugated goat anti-rabbit IgG second antibody was used in all three cases (1:600), incubated for 1 hour at room temperature. The staining was developed by incubation for 15 minutes with 0.6% diaminobenzidine followed by addition of H_2O_2 and incubation for 4 minutes. After immunostaining, all sections were mounted on gelatin-coated glass, air-dried, dehydrated in ascending concentrations of ethanol, cleared with xylene, and coverslipped with Canada balsam (Merck, Darmstadt, Germany).

Nissl, CR, and Th-S Fluorescence Staining

Mounted sections were defatted in xylene and hydrated in ethyl alcohol and water series. Nissl staining (cresyl violet) was performed as previously described.[33] CR staining using alkaline CR methods was performed as previously described.[35] Th-S staining was performed as described by Elghetany and Saleem.[34]

Image and Statistical Analysis

All histological and immunohistochemical images were acquired from a Zeiss Axioplan microscope with a 35-mm camera system. To analyze all plaque-like deposits in one field, ×10 and ×20 optical magnifications were used. The pictures were digitalized in a Nikon Coolscan III Scanner, and each image was routed into a PC-compatible microcomputer via Adobe-Photoshop program (5.5). Once digitalized, the images were analyzed with Scion Image public domain software (Scion Image for Windows β 4.02, on the internet at *http://www.scioncorp.com*). Custom macro subroutine was used to calculate positively stained areas, of both immunopositives stain-

ing for Aβ Th-S-fluorescence and CR-positive deposits. The same slides were analyzed single blind by two different investigators to ensure that trends were independent of individual bias. Serial coronal sections of the hippocampus were performed between the coordinates in an anteroposterior location to the injection site. The parameter measured was the positive area stained in six 50-μm-thick sections per rat per assay. Results from this analysis revealed the average of total area of the deposit. Analysis of number of cells, GFAP and laminin staining area, and GFAP intensity were measured with SigmaScan Pro software. Data from the image analysis macros were exported to a Sigma Plot file for statistical analysis. Results were expressed as mean ± SE. Statistical significance was determined by one-way analysis of variance.

Results

Aβ and Aβ-AChE Complexes after Intrahippocampal Injections

A specific antibody against the Aβ peptide revealed successful injection of Aβ fibrils into the dorsal hippocampus. Anti-Aβ immunohistochemistry showed clear accumulation of Aβ-positive deposits after intrahippocampal injection of Aβ fibrils assembled with and without AChE. These deposits were observed in animals after 2 (Figure 1, A and B) and 8 weeks (Figure 2, D and G). Significant differences in the size of the deposits between both treatment groups were observed after 8 weeks of treatment using three different staining methods, anti-Aβ antibody, thioflavine S, and CR (Figure 2J). In fact, animals examined at 2 weeks showed similar size of the Aβ immunopositive areas with both injection treatments (Figure 1G), however, when animals were examined after 8 weeks of injection, a significant increase in the size of Aβ-immunopositive area was observed in the case of animals injected with Aβ-AChE complexes. This was evident after performing a digital quantification of the hippocampal areas stained with the anti-Aβ antibody, which indicated almost a threefold increase of amyloid load in animals co-injected with Aβ-AChE complexes compared with Aβ (Figure 2J). Control animals injected with an unrelated peptide sequence derived from the β-APP gave no specific amyloid staining (data not shown).

To verify that Aβ deposits were in fact amyloid-positive, we performed two well-known specific and sensitive staining procedures: Th-S-fluorescence and polarized light microscopy after CR staining under polarized light. We observed that extracellular deposits positive for an antibody against the Aβ peptide were indeed positive for Th-S-fluorescence (a 2.5-fold increase, Figure 2J), in a similar way to very dense amyloid cores observed in AD lesions[36,37] with the same pattern of anti-Aβ staining in both treatment groups (compare Figure 1, C and D, with A and B, respectively; and Figure 2, E and H, with D and G, respectively). However, in all animals injected with Aβ-AChE complexes, examined at 8 weeks after injection, amyloid deposits were larger in size with respect to animals injected with Aβ fibrils assembled alone (Figure 2, E *versus* H), confirming the results obtained with anti-Aβ immunostaining (see also for digital quantification, Figure 2J). Control animals injected with vehicle alone were completely negative for amyloid-specific staining (Figure 2; A to C). In general, samples were observed under cross-polarized light microscopy after CR staining under polarized light is normally used, two kinds of positive staining are observed, one of these corresponds to an apple green birefringence, and the other, to a compact stellate staining, resembling Maltese crosses; the difference in staining is however poorly understood.[38] Aβ-positive deposits observed in both groups proved to be positive for CR staining (Figure 1, E and F; Figure 2, F and I), CR amyloid deposits were indicative of fibrillar amyloid deposition. In these cases, the congophilic aggregates were similar in size and stained with CR showing a compact congophilic material rounded by apple green birefringent deposits 2 weeks after injection (Figure 1G). However, in animals examined 8 weeks after injection, amyloid deposits showed differences between both groups. Rats injected with the Aβ-AChE complexes

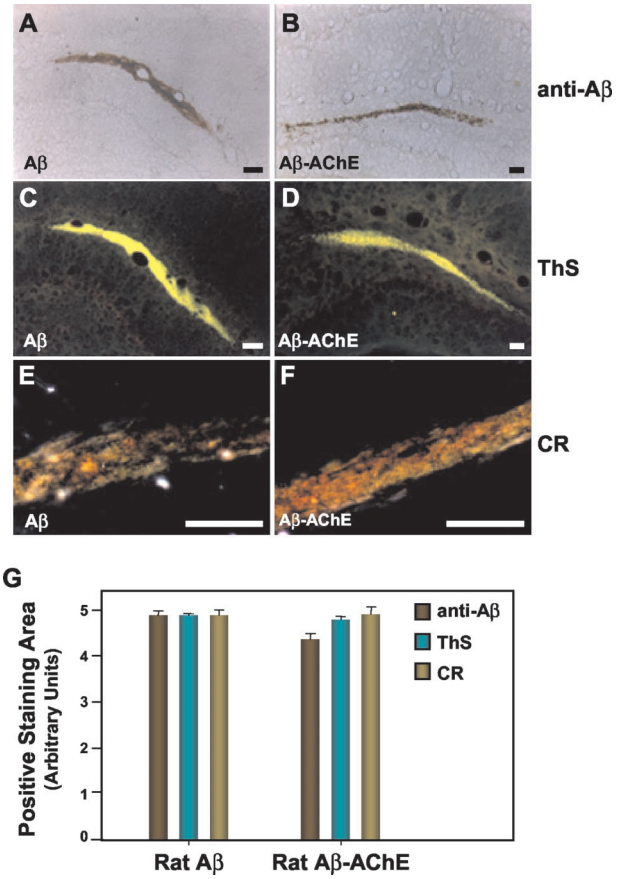

Figure 1. Aβ deposit detection *in situ* in animals injected with Aβ and Aβ-AChE complexes 2 weeks after injection. Anti-Aβ immunostaining of coronal sections from animals injected with Aβ fibrils and Aβ-AChE complexes (**A** and **B**, respectively). Th-S fluorescence of corresponding sections (**C** and **D**) and CR staining viewed under polarized light (**E** and **F**). **G:** Digital quantification of positively stained areas of sections stained with antibody against Aβ, Th-S fluorescence, and CR were measured with the SigmaScan Pro. The analysis revealed the total average area of the deposit. Data from the image analysis macroscopy were exported to a Sigma plot file for statistical analysis. Results were expressed as mean ± SE. Scale bars: 100 μm (**A–D**); 50 μm (**E**, **F**).

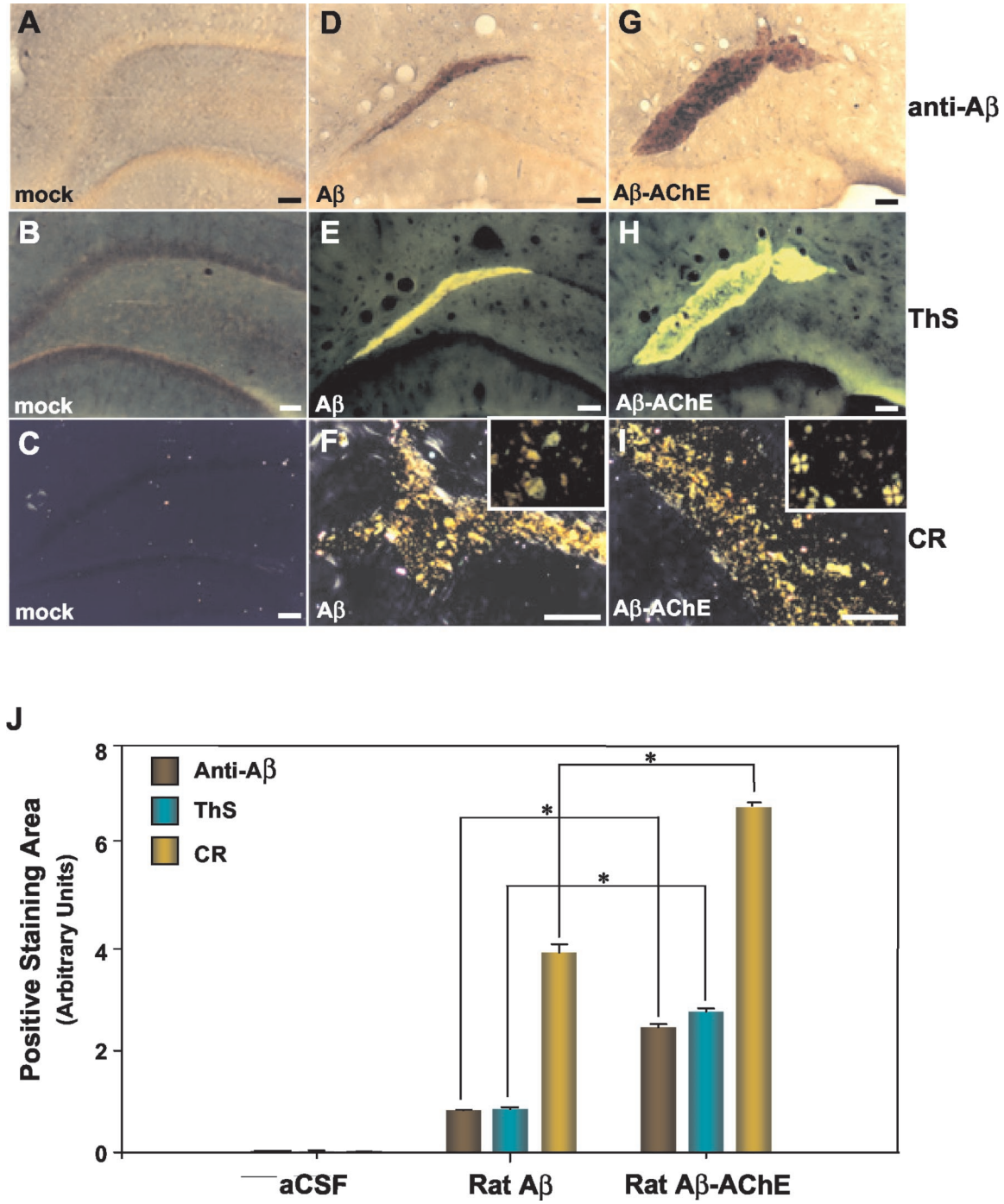

Figure 2. Aβ deposits and amyloid detection *in situ* in animals 8 weeks after injection. Anti-Aβ immunostaining of a coronal section from animals injected into hippocampus with ACF, Aβ fibrils, and Aβ-AChE complexes, Th-S fluorescence of the corresponding sections, and CR staining under polarized light. **D**, **E**, and **F:** Staining of sections from animals injected with Aβ fibrils that maintain immunopositive Aβ deposits (**D**), amyloid-positive as shown by Th-S (**E**)- and CR (**F**)-specific staining. **G**, **H**, **I:** The brain slides from animals injected with Aβ-AChE complexes are also immunopositive for Aβ deposits using an anti-Aβ antibody; however these deposits are larger than those observed in rats injected with Aβ fibrils (**G**). These Aβ deposits are amyloid-positive as shown by Th-S fluorescence (**H**) and CR (**I**) staining. Note that the amyloid deposits obtained with Aβ-AChE complexes stained with CR, present birefringent deposits and Maltese cross-positive pattern (**I**, **inset**), in contrast, rats injected with Aβ fibrils did not present Maltese crosses (**F**, **inset**). **J:** The graph corresponds to a digital quantification (SigmaScan Pro) of the amyloid deposits shown above (see Figure 1G and Material and Methods). Results were expressed as mean ± SE. Statistical significance was determined by one-way analysis of variance; *, $P < 0.05$ was regarded as statistically significant. Scale bars: 100 μm (**A–E**, **G**, **H**); 50 μm (**F**, **I**).

exhibit amyloid deposits in which CR Maltese crosses are easily distinguished on microscopic observation (Figure 2I, inset), apple green birefringent deposits were also present. Those animals injected with Aβ fibrils only showed green apple birefringent deposits corresponding to amyloid, and they did not exhibit Maltese crosses (Figure 2F, inset). AD lesions have been well characterized in terms of this feature, and the CR Maltese cross staining has been recognized in these particular lesions.[38,39] The fact that both groups exhibit amyloid de-

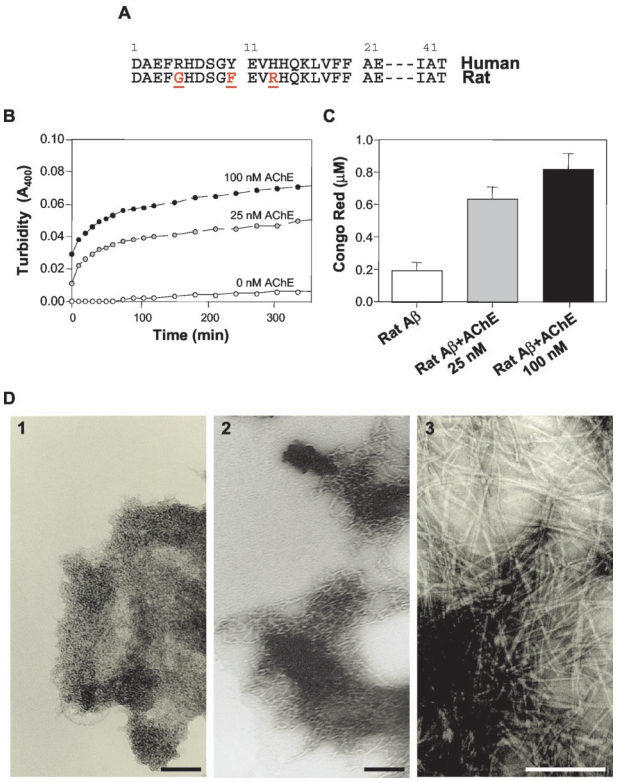

Figure 3. AChE induces the aggregation of rat Aβ into Alzheimer's amyloid fibrils. **A:** Human and rat Aβ sequence, showing the difference in amino acids 5, 10, and 13. **B:** Turbidity kinetic aggregation assay of rat Aβ alone (**white circles**) or in the presence of 25 nmol/L (**gray circles**) and 100 nmol/L AChE (**black circles**). **C:** CR binding assay performed after 24 hours of incubation showed that similar amounts of amyloid were formed with both AChE concentrations used. **D:** Electron microscopy of amyloid fibrils obtained from rat $A\beta_{1-40}$ (**1**), rat $A\beta_{1-40}$ plus 100 nmol/L AChE (**2**), and human 100 μmol/L $A\beta_{1-40}$ (**3**).

posits with these subtle differences suggests that the presence of AChE in the amyloid plaques makes the difference.

AChE Accelerates Aggregation of Rat Aβ

The fact that 8 weeks later the animals injected with Aβ-AChE complexes showed an increment in the size of the Aβ deposit suggests that the endogenous rat Aβ peptide might be recruited to the newly formed plaque, probably through the influence of AChE. To evaluate whether AChE was able to induce *in vitro* the rat Aβ peptide assembly in Alzheimer-type of amyloid aggregates, a synthetic rat $A\beta_{1-40}$ peptide (Figure 3A) was used to study the effect of pure AChE in an Aβ aggregation assay. Turbidity assays show that AChE induces rat Aβ peptide to form amyloid fibrils in an AChE concentration-dependent manner (Figure 3B) as shown by CR-binding measurements (Figure 3C) to confirm that the aggregates correspond to amyloid. An electron microscopic study was performed to establish the formation of amyloid fibrils from the assembly of rat $A\beta_{1-40}$ peptide, in the presence and absence of increasing AChE. Figure 3D shows, that AChE stimulates the amyloid fibril formation of the rat $A\beta_{1-40}$ peptide in comparison with the rat Aβ peptide alone.

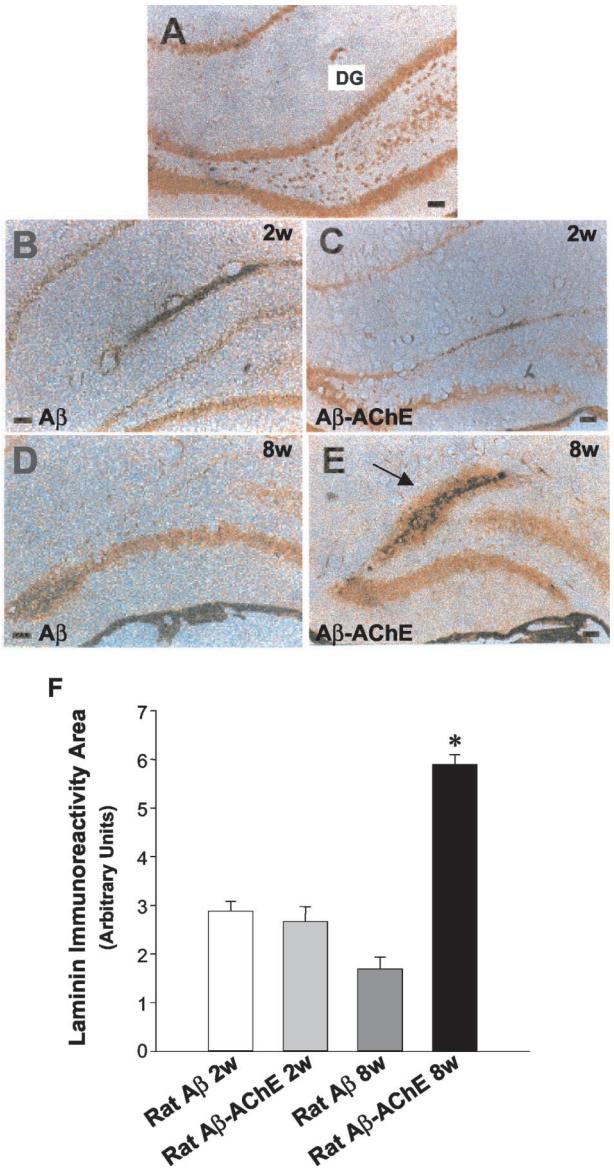

Figure 4. Laminin immunoreactivity of amyloid deposits induced by Aβ-AChE complexes. **A:** Laminin is detected in the hippocampus associated to pyramidal neurons in the dentate gyrus in intact control animals. This immunoreactivity is focally diminished in the DG after 2 weeks of injection with Aβ fibrils (**B**) and with Aβ-AChE complexes (**C**). These results were maintained, after 8 weeks, in those animals injected with Aβ fibrils (**D**). However, in rats injected with Aβ-AChE complexes, the immunostaining was extensive (**E**) and it was concentrated extracellularly in the injection site (**arrow**), a fact that was not observed in the other groups. **F:** Laminin-immunoreactive area was quantified with the SigmaScan Pro software in adjacent brain sections. As observed in the graph, animals injected with Aβ-AChE complexes present a significant increase in laminin staining associated to the amyloid deposit in comparison to those injected with Aβ fibrils, 8 weeks after injection. *, $P < 0.05$. Scale bars, 100 μm.

Aβ-AChE Complexes Recruit Laminin to Amyloid Deposits

Laminin is a normal component of the extracellular matrix, which is found in the brain lesions of patients with AD and

Down's syndrome.[40,41] To further characterize the lesions induced by the injected amyloid, we performed immunohistochemical analysis using an anti-laminin polyclonal antibody (Figure 4). At 2 weeks after injection, the characterization of injected amyloid deposits formed with Aβ alone or Aβ-AChE complexes showed little laminin immunoreactivity along the dentate gyrus (Figure 4; A to C). Laminin stain changes considerably 8 weeks after injection. Animals injected with Aβ fibrils alone showed very little laminin immunostaining associated to amyloid deposits (Figure 4D), but lesions induced by Aβ-AChE complexes showed an increased laminin immunoreactivity associated with the core of amyloid deposits in all of the animals examined after 8 weeks (Figure 4E, arrow), suggesting that more laminin was attracted to the Aβ-AChE complexes, as a result of the laminin increases observed after injury.[11] The quantification of the laminin staining area in the upper leaf of the dentate gyrus shows that the presence of Aβ-AChE complexes induces a clear increase in laminin immunoreactivity 8 weeks after injection (Figure 4F), in the region associated with the amyloid deposit (Figure 4E). To characterize the interaction between laminin and the induced amyloid deposits, $A\beta_{1\text{-}40}$ soluble peptide was infused concomitantly with AChE into the hippocampus. After 2 weeks of infusion, animals were sacrificed and coronal brain sections were analyzed for the presence of amyloid deposits with Th-S and adjacent sections were submitted to laminin detection (Figure 5). As observed in Figure 5A, a big Th-S-positive plaque was detected in the animal. Interestingly, surrounding the amyloid plaque a clear laminin staining was observed (Figure 5B, arrowheads), which corresponds to hippocampal neurons with increased laminin immunoreactivity (Figure 5B, arrows in the inset). The results suggest that laminin is induced in adult rat brain by injury, in the boundaries of the amyloid plaque.

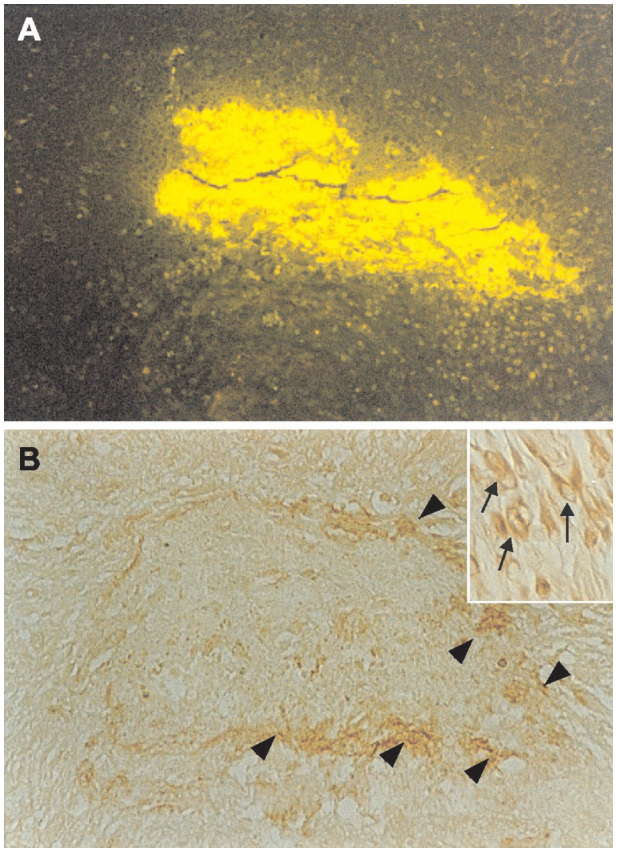

Figure 5. Neurons that express laminin appear around the newly formed amyloid-AChE plaque. Animals were infused using an Alzet miniosmotic pump for 4 weeks with $A\beta_{1\text{-}40}$ soluble peptide plus AChE into the hippocampus. **A:** Brain sections analyzed with Th-S present a big Th-S-positive deposit as a result of the infusion. **B:** Interestingly, adjacent sections showed laminin staining around the amyloid deposit (**arrowheads**) that correspond to neurons with increased laminin immunoreactivity (**inset**, **arrows**). Original magnifications: ×10; ×100 (**inset**).

Laminin Depolymerizes Aβ Fibrils, but Not Aβ-AChE Complexes

One possible explanation for the presence of laminin in the amyloid deposits that contain AChE may be related to the fact that laminin was induced and secreted toward the amyloid deposits, to depolymerize amyloid fibrils, as has been previously reported.[42–44] However, in view that an extensive amyloid deposition was observed in brains injected with Aβ-AChE complexes, we analyzed the ability of laminin to disaggregate AChE-containing amyloid deposits *in vitro*. For such a purpose we prepared $A\beta_{1\text{-}40}$ fibrils either in the presence or absence of AChE (molar ratio, AChE: Aβ = 1:1000). In Figure 6, 200 nmol/L of laminin completely disaggregated 100 μmol/L of Aβ fibrils in 2 hours at room temperature (Figure 6, white circles) but in the presence of 100 nmol/L of AChE this effect was not observed (Figure 6, white inverted triangles). Aβ fibrils and Aβ-AChE complexes remained unchanged in the absence of laminin (Figure 6, black circles and inverted triangles, respectively). The inset of Figure 6 shows the Aβ fibril (Th-T fluorescence) dependence on laminin concentration in the presence or absence of AChE at 2 hours of incubation.

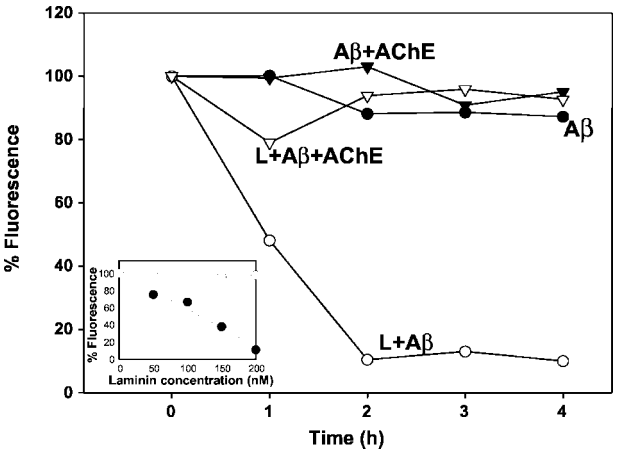

Figure 6. Laminin disaggregates Aβ fibrils, but not Aβ-AChE complexes *in vitro*. $A\beta_{1\text{-}40}$ fibrils (100 μmol/L) prepared either in the absence (**circles**) or the presence (**inverted triangles**) of AChE at a molar ratio of 1:1000 = AChE:Aβ were incubated either with 200 nmol/L of laminin (**white symbols**) or vehicle (**black symbols**). Th-T fluorescence (as expressed as percentage of respective time 0 points) of samples was taken at indicated time points. The **inset** shows the laminin concentration dependence of Th-T fluorescence formed in the presence (**white circles**) or the absence (**black circles**) of AChE at 2 hours of the assay.

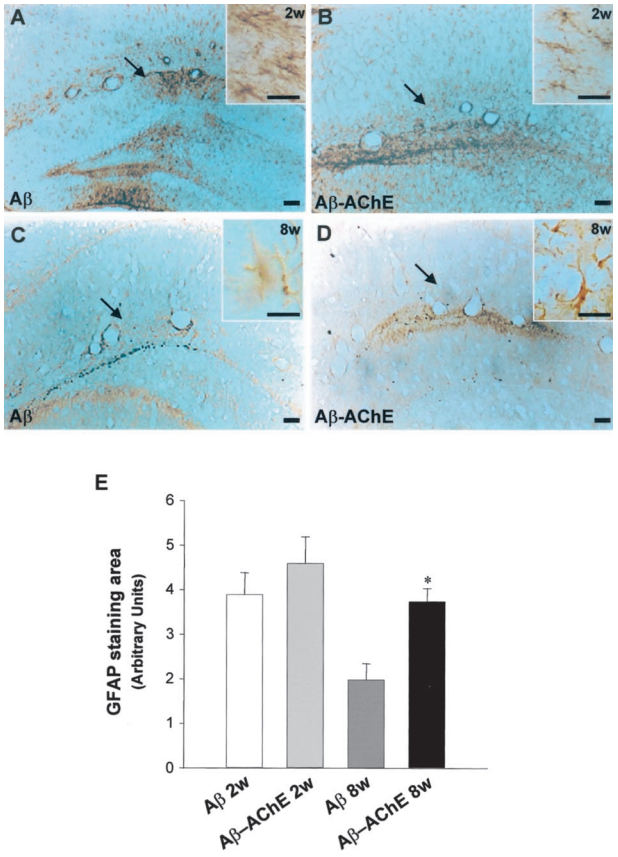

Figure 7. Astrocytosis induced by Aβ fibrils and Aβ-AChE complex injections into the hippocampus. Immunostaining using anti-GFAP of coronal sections from animals injected with Aβ fibrils, 2 weeks and 8 weeks after injection (**arrows** indicate the injection site). **A** and **C:** Anti-GFAP immunodetection in injected brains with Aβ fibrils at 2 (**A**) and 8 (**C**) weeks after injection. **B** and **D:** Anti-GFAP immunodetection in brain sections from animals injected with Aβ-AChE complexes, 2 (**B**) and 8 weeks (**D**) after injection. Higher magnification shows the characteristic stellate morphology of the astrocytes (**insets** in **A** and **B**). E**:** GFAP staining at 2 and 8 weeks after injection. GFAP immunoreactivity area was quantified (SigmaScan Pro), confirming that rats injected with Aβ-AChE complexes present an increased GFAP staining *, $P < 0.05$. Scale bars: 100 μm (**A–D**); 20 μm (**insets**).

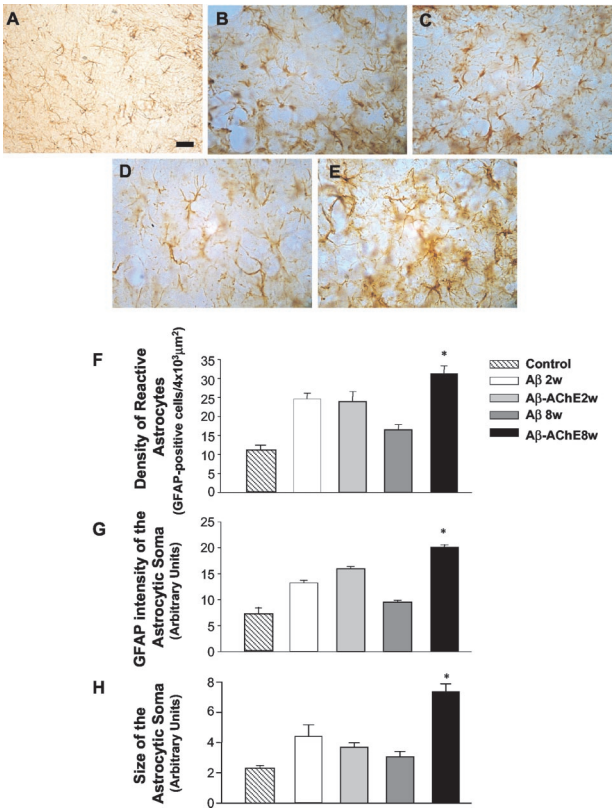

Figure 8. Aβ-AChE complexes induced the appearance of hypertrophic astrocytes. A more exhaustive analysis of the upper leaf of the dentate gyrus allowed us to characterize the reactive astrocytes found in the injection site. **A:** Control astrocytes in animals injected with ACF+DMSO (control). Animals treated with Aβ fibrils and without AChE (**B**) and with AChE (**C**) present some reactive astrocytes at 2 weeks. However, 8 weeks after injection those animals injected with Aβ fibrils showed a decreased GFAP immunoreactivity (**D**), in contrast with those injected with Aβ-AChE complexes, which showed more intense reactive astrocytes (**E**). The density of reactive astrocytes, intensity of staining, and size of the astrocyte soma were quantified (SigmaScan Pro) (**F–H**). The graph shows a decreased density of astrocytes in rats injected with Aβ fibrils 8 weeks after injection; in contrast those injected with Aβ-AChE complexes show an increased density of reactive astrocytes. GFAP intensity staining as well as the size of the cell body was quantified (SigmaScan Pro) (**F**, **G**). The presence of AChE induced the appearance of hypertrophic signals as an increased GFAP intensity in the soma (**G**) and an enhanced size of the astrocyte soma after 8 weeks of treatment indicating astrocyte hypertrophy (**H**). Original magnifications, ×40. Scale bars: 100 μm (**A–E**). *, $P < 0.05$ (Student's *t*-test; **F–H**).

Aβ and Aβ-AChE Complexes Induce GFAP-Positive Astrocytes, but Only the Aβ-AChE Complexes Induced Reactive Hypertrophic Astrocytes

It is well known that reactive astrocytes are an indication of inflammatory processes that occur in response to brain injury.[45] In the present study, we used GFAP immunoreactivity to visualize the cellular response of glial cells to the injection treatments. Reactive astrocytes were observed near to the injection site at 2 and 8 weeks after injection (Figure 7). In the case of animals injected with Aβ fibrils the astrocytic responses returned to the basal levels after 8 weeks of injection (Figure 7, A and C) in a similar manner as observed after $A\beta_{25\text{-}35}$ fragment injection.[46] Animals injected with Aβ-AChE complexes showed GFAP staining closely associated to the amyloid deposits (see below) (Figure 7, B and D). The GFAP-stained area in the injection site was quantified (Figure 7E). As observed in the graph, Aβ fibrils and Aβ-AChE complexes induced an astrocytic response after 2 weeks of treatment; after 8 weeks of treatment, the astroglial response area decreased importantly in the Aβ fibrils injected rats, in contrast to those animals injected with Aβ-AChE complexes, which maintained an increased GFAP immunoreactivity area (Figure 7E). In all of the cases sections were obtained at comparable distances from the injection site. The activation of astrocytes was better observed in Figure 8. The injection of either Aβ fibrils or Aβ-AChE complexes did induce some astrocytosis 2 weeks after the injection (Figure 8, B and C); however, at 8 weeks after the injection, the astrogliosis apparently diminished in Aβ fibrils in injected rats (Figure 8D) more dramatically than in rats injected with Aβ-AChE complexes, which show hypertrophic highly reactive astrocytes (Figure 8E). The analysis of the upper leaf of the dentate gyrus of the hippocampus allowed us to quantify

the reactive astrocytes as GFAP-positive cells in that region. Eight weeks after injection the number of reactive astrocytes augmented 200% in animals injected with Aβ-AChE complexes as compared with animals injected only with Aβ fibrils (Figure 8F). Likewise, the GFAP intensity in the astrocyte soma was measured. Animals injected with Aβ-AChE complexes showed a significant increment in the intensity of GFAP immunostaining compared with those animals injected with Aβ fibrils 8 weeks after injection (Figure 8G). Finally, we measured the size of the astrocyte soma found in the dentate gyrus; in agreement with the previous results, after 8 weeks of treatment, reactive astrocytes present an increase in the size of the cellular soma in response to Aβ-AChE complexes (Figure 8H), confirming the presence of hypertrophic reactive astrocytes in rats injected with Aβ-AChE complexes. All of the treatments showed a higher astrogliosis than the control (ACF+DMSO) (Figure 8A), however, only the reactive response triggered by the Aβ-AChE complex increased with time. These results suggest that the return to basal levels of the astrocytic response is delayed in animals injected with Aβ-AChE complexes, probably because of the presence of a more toxic environment than the one of animals injected with Aβ fibrils alone.

Aβ and Aβ-AChE Complexes Induce Neuronal Cell Loss, but the Effect of the Aβ-AChE Complexes Was More Evident

Neuronal cell loss was examined by using a specific neuronal stain, cresyl violet, which did not stain glial cells.[33] Sections of the dorsal hippocampal region stained with cresyl violet (Nissl stain) showed that the injection of Aβ fibrils, assembled alone or in the presence of AChE induces loss of granular neurons involving mainly the upper leaf of the dentate gyrus near the injection site (Figure 9; C to F), in contrast to intact (Figure 9A), mock injected (ACF, picture not shown) or to control injected rats (ACF plus DMSO) (Figure 9B, control), which showed no degeneration in the same area (Figure 9B). This latter observation indicates that neither the injection per se nor the mechanical procedures accompanying surgery induce neuronal degeneration or cell death. Neuronal cell loss was visualized by the thickness or the absence of the Nissl staining in the dentate gyrus of the hippocampus. The number of neuronal losses appears similar in animals treated with Aβ fibrils and Aβ-AChE complexes during the first 2 weeks, however the total number of neurons in treated animals decreased in almost 50% respect to the control (Figure 9, C and D, respectively). However, after 8 weeks of injection a major degenerative effect was observed in animals injected with Aβ-AChE complexes in comparison with those injected with Aβ fibrils alone (compare Figure 9, E *versus* F). Coronal brain sections stained with Nissl staining of different animals were quantified and the number of neuronal cells present along the dentate gyrus estimated. Results are presented in Figure 9G. It is clear that the injection of both Aβ fibrils and Aβ-AChE complexes, induces at 2 weeks, a significant neuronal cell loss (almost

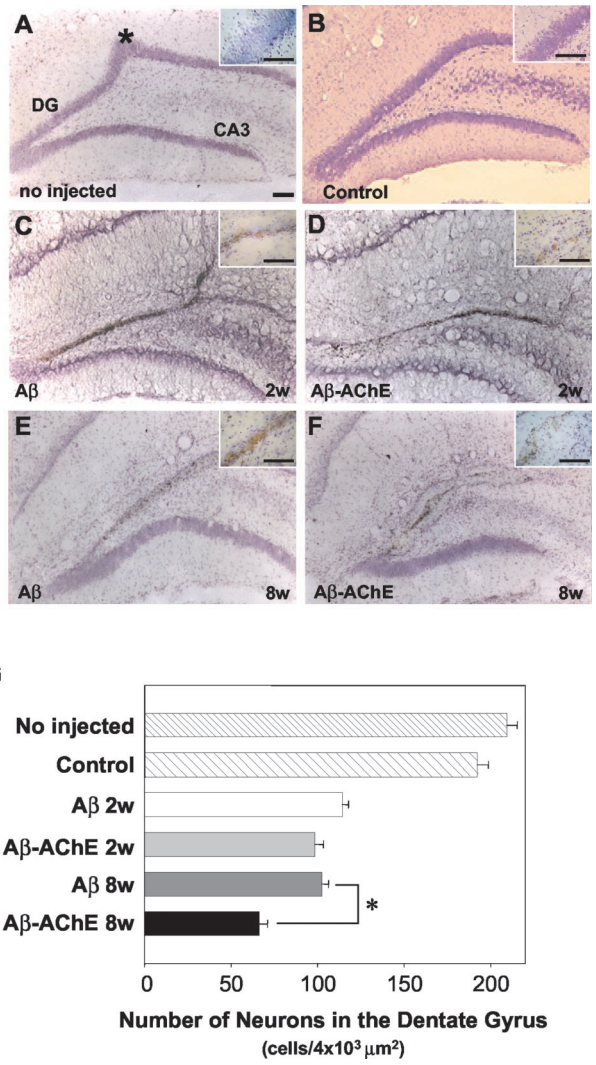

Figure 9. Nissl staining (cresyl violet) at 2 and 8 weeks after Aβ fibril and Aβ-AChE complex injections. Nissl stained coronal sections through dorsal hippocampus near to the injection site (*) (intact animal **A**) in bilaterally injected rats with ACF+DMSO (control). DG indicates the dentate gyrus and CA3 indicates the region of the Ammon horn of the hippocampus (**B**), Aβ fibrils assembled alone after 2 (**C**) and 8 weeks (**E**), and Aβ-AChE complexes after 2 (**D**) and 8 weeks (**F**). Note the extensive neuronal degeneration in animals injected with Aβ-AChE complexes after 8 weeks. **G:** Pictures (×40) of Nissl-stained sections were submitted to quantification of the neuron number. As observed in the graph, only Aβ-AChE complexes after 8 weeks of treatment induced a significant neuronal cell loss in the upper leaf of the dentate gyrus. *, $P > 0.05$ (Student's *t*-test). Scale bars, 100 μm.

50% of control animals), however, at 8 weeks after injection, the Aβ-AChE complexes induced a further and more pronounces decrease in neuronal cell loss. These results indicate, again, that a more drastic effect of the Aβ-AChE amyloid deposits was apparent at the level of the number of neurons present at the dentate gyrus of the hippocampus.

Discussion

In the present study we have demonstrated that the intrahippocampal injection of Aβ-AChE complexes in the rat induced the formation of amyloid deposits *in vivo* that are different from the ones generated after the injection of

Aβ fibrils alone, by size, laminin content, and CR staining. Moreover, amyloid deposits formed after injection of Aβ-AChE complexes share some important characteristics with amyloid deposits actually found in AD brains, including extensive astrocytosis, neuronal cell loss, recruitment of laminin to amyloid deposits, and the Maltese cross pattern observed under cross-polarized light.[38,39]

Our results are reminiscent of the previous studies carried by Snow and colleagues,[39] in which they demonstrated plaque formation *in vivo* using co-infusion of Aβ with heparan sulfate proteoglycans, moreover they found that Aβ injected with the proteoglycan was more stable and more fibrillogenic than Aβ injected alone.

In our study the presence of the Aβ peptide was detected with a polyclonal antibody against the human $A\beta_{1\text{-}40}$ sequence, which recognized rat Aβ in Western blot (data not shown). Interestingly, after 2 weeks of treatment, no differences in the size of amyloid deposits between animal groups were observed. However, 8 weeks after injection, amyloid deposits were significantly larger in animals treated with Aβ-AChE complexes than those treated with Aβ fibrils. These observations were confirmed by measuring the Th-S fluorescence-positive area. Because the starting material was the same for both treatment groups, it is conceivable that Aβ-AChE complexes could recruit endogenous Aβ peptide, because of the presence of AChE incorporated in amyloid fibrils. This possibility is likely, because, we have previously shown that AChE was able to accelerate the assembly of the Aβ peptide into Alzheimer-type of amyloid fibrils.[21] In fact, in the present work we were able to demonstrate that AChE was indeed able to promote rat Aβ peptide aggregation into amyloid fibrils *in vitro*, despite the very low intrinsic aggregation capacity of the rat Aβ peptide, because rat Aβ peptide has three amino acid substitutions in relation to the human Aβ sequence.[47] Histological analysis of rat brain serial sections stained with CR showed that the injected material was congophilic and produced birefringence under polarized light. Notably, animals injected with Aβ-AChE complexes exhibited the Maltese cross pattern within amyloid deposits, suggesting that this amyloid was somehow different from the one resulting from injection of Aβ fibrils alone, and reminiscent of the real AD lesions. It is possible that these differences may be because of a different composition, originating from the incorporation of endogenous elements including proteins and metals.

The role of laminin in AD brains has been associated with the growth of neuronal processes.[40] However, we and others had shown that laminin could be involved in the inhibition of amyloid formation *in vitro*[48–50] and we had demonstrated that preformed amyloid fibrils could be depolymerize *in vitro.*[42–44] The presence of laminin close to the amyloid deposits may indicate a sort of defense mechanism in which laminin may initiates the depolymerization of Aβ fibrils, however, the fact that laminin remains associated to the amyloid deposits, without destroying them, may mean that in the presence of AChE, the amyloid fibrils became more resistant to the effect of laminin. This possibility was examined *in vitro* and proves to be true, ie, in the presence of AChE, Aβ fibrils became resistant to laminin depolymerization.

To assess whether amyloid deposits induced neuronal cell death in rat brains, we examined serial tissue sections of the dentate gyrus using the Nissl technique. Two weeks after an acute injection, no morphological differences between both groups were found, and the extent of neuronal cell loss was concentrated in the upper leaf of dentate gyrus, and it was similar in both cases. The neuronal cell loss observed is similar in animals treated with Aβ fibrils (2 and 8 weeks) and Aβ-AChE complexes (2 weeks), showing more than 35% neuronal loss respect to controls, which is reminiscent of the neuronal cell loss in dentate and hippocampal fissure observed after human amyloid cores injection, at similar coordinates.[51] However, at 8 weeks after injection, the Aβ-AChE complexes induced a further and more pronounced decrease in neuronal cell loss (more than 50% cell loss). Similar results have been obtained previously in our laboratory using infusion models.[52–54] Our finding indicates that the damage induced by the injection of Aβ-AChE complexes was specific and not related to mechanical disruption. Some authors have suggested that the vehicle used to dissolve Aβ peptide could be a determinant factor in the damage induced by the injection,[55] in our study this possibility was ruled out, because we rinsed the Aβ fibrils exhaustively and then they were resuspended in ACF before the stereotaxic injections were performed.

The mechanisms of *in vivo* toxicity of β-amyloid are not completely understood, however there is evidence indicating that adult rats injected into the basal forebrain with the Aβ peptide undergo a decrease in acetylcholine release from the hippocampus.[56] Other authors have demonstrated that intracerebral injections of $A\beta_{1\text{-}40}$ in rat brain, determined neuronal cell loss in the cholinergic system, as well as an extracellular accumulation of AChE.[57] Similar approaches have shown that the intracerebral administration of $A\beta_{1\text{-}42}$ produced toxic effects in cholinergic neurons as indicated by a decrease in choline acetyltransferase (ChAT) immunoreactive neurons in the basal forebrain together with a reduction in ChAT-positive axons in the cerebral cortex.[58]

In conclusion, our studies are consistent with the notion that Aβ-AChE complexes trigger some of the neurodegenerative changes observed in AD brain, and that AChE may potentiate not only the amyloid deposition *in vivo*, but also the toxicity of the amyloid deposits. Finally, recent studies obtained with a double-transgenic mice that overexpress human AChE and APP are consistent with the results presented here, in fact, double-APP-AChE transgenic mice showed amyloid plaques earlier than those animals overexpressing APP alone.[59]

References

1. Salmon DP, Bondi MW: Neuropsychology of Alzheimer disease. Alzheimer Disease. Edited by RD Terry, R Katzman, KL Bick, SS Sisodia. Philadelphia, Lippincott Williams & Wilkins, 1999, pp 39–56
2. Glenner GG: The pathobiology of Alzheimer's disease. Annu Rev Med 1989, 40:45–51

3. Selkoe DJ: Alzheimer's disease: genes, proteins, and therapy. Physiol Rev 2001, 81:741–766
4. Itagaki S, McGeer PL, Akiyama H, Zhu S, Selkoe D: Relationship of microglia and astrocytes to amyloid deposits of Alzheimer disease. J Neuroimmunol 1989, 24:173–182
5. Selkoe DJ: The molecular pathology of Alzheimer's disease. Neuron 1991, 6:487–498
6. Roher A, Wolfe D, Palutke M, KuKuruga D: Purification, ultrastructure, and chemical analysis of Alzheimer disease amyloid plaque core protein. Proc Natl Acad Sci USA 1986, 83:2662–2666
7. Namba Y, Tomonaga M, Kawasaki H, Otomo E, Ikeda K: Apolipoprotein E immunoreactivity in cerebral amyloid deposits and neurofibrillary tangles in Alzheimer's disease and kuru plaque amyloid in Creutzfeldt-Jakob disease. Brain Res 1991, 541:163–166
8. Abraham CR, Selkoe DJ, Potter H: Immunochemical identification of the serine protease inhibitor α1-antichymotrypsin in the brain amyloid deposits of the Alzheimer's disease. Cell 1988, 52:487–501
9. Kalaria RN, Kroon SN, Grahovac I, Perry G: Acetylcholinesterase and its association with heparan sulphate proteoglycans in cortical amyloid deposits of Alzheimer's disease. Neuroscience 1992, 51:177–184
10. Snow AD, Sekiguchi RT, Nochlin D, Kalaria RN, Kimata K: Heparan sulfate proteoglycan in diffuse plaques of hippocampus but not of cerebellum in Alzheimer's disease brain. Am J Pathol 1994, 144: 337–347
11. Liesi P, Kaakkola S, Dahl D, Vaheri A: Laminin is induced in astrocytes of adult brain by injury. EMBO J 1984, 3:683–686
12. Geula C, Mesulam M: Special properties of cholinesterases in the cerebral cortex of Alzheimer's disease. Brain Res 1989, 498:185–189
13. Ulrich J, Meier-Ruge W, Probst A, Meier E, Ipsen S: Senile plaques: staining for acetylcholinesterase and A4 protein. A comparative study in the hippocampus and entorhinal cortex. Acta Neuropathol 1990, 80:624–628
14. Kasa P, Rakonczay Z, Gulya K: The cholinergic system in Alzheimer's disease. Prog Neurobiol 1997, 52:511–535
15. Whitehouse PJ, Price DL, Struble RG, Clark AW, Coyle JT, Delon MR: Alzheimer's disease and senile dementia: loss of neurons in the basal forebrain. Science 1982, 215:1237–1239
16. Talesa VN: Acetylcholinesterase in Alzheimer's disease. Mech Ageing Dev 2001, 122:1961–1969
17. Arendt T, Bigl V, Tennesdt A, Arendt A: Neuronal loss in different parts of the nucleus basalis is related to neuritic plaque formation in cortical target areas in Alzheimer's disease. Neuroscience 1985, 14:1–14
18. Beeri R, Andres C, Lev-Lehman E, Timberg R, Huberman T, Shani M, Soreq H: Transgenic expression of human acetylcholinesterase induces progressive cognitive deterioration in mice. Curr Biol 1995, 5:1063–1071
19. Beeri R, Le Novere N, Mervis R, Huberman T, Grauer E, Changeux JP, Soreq H: Enhanced hemicholinium binding and attenuated dendrite branching in cognitively impaired acetylcholinesterase-transgenic mice. J Neurochem 1997, 69:2441–2451
20. Sternfeld M, Shoham S, Klein O, Flores-Flores C, Evron T, Idelson GH, Kitsberg D, Patrick JW, Soreq H: Excess "read-through" acetylcholinesterase attenuates but the "synaptic" variant intensifies neurodeterioration correlates. Proc Natl Acad Sci USA 2000, 97:8647–8652
21. Inestrosa NC, Alvarez A, Perez CA, Moreno RD, Vicente M, Linker C, Casanueva OI, Soto C, Garrido J: Acetylcholinesterase accelerates assembly of amyloid-β-peptides into Alzheimer's fibrils: possible role of the peripheral site of the enzyme. Neuron 1996, 16:881–891
22. De Ferrari GV, Canales MA, Shin I, Weiner LM, Silman I, Inestrosa NC: A structural motif of acetylcholinesterase that promotes amyloid β-peptide fibril formation. Biochemistry 2001, 40:10447–10457
23. Alvarez A, Opazo C, Alarcón R, Garrido J, Inestrosa NC: Acetylcholinesterase promotes the aggregation of amyloid-β-peptide fragments by forming a complex with the growing fibrils. J Mol Biol 1997, 272:348–361
24. Alvarez A, Alarcon R, Opazo C, Campos EO, Muñoz FJ, Calderón FH, Dajas F, Gentry MK, Doctor BP, De Mello FG, Inestrosa NC: Stable complexes involving acetylcholinesterase and amyloid-β peptide change the biochemical properties of the enzyme and increase the neurotoxicity of Alzheimer's fibrils. J Neurosci 1998, 18:3213–3223
25. Muñoz FJ, Inestrosa NC: Neurotoxicity of acetylcholinesterase-amyloid β-peptide aggregates is dependent on the type of Aβ peptide and the AChE concentration present in the complexes. FEBS Lett 1999, 450:205–209
26. Muñoz FJ, Opazo C, Gil-Gómez G, Tapia G, Fernández V, Valverde MA, Inestrosa NC: Vitamin E but not 17β-estradiol protect against vascular toxicity induced by β-amyloid wild-type and the Dutch amyloid variant. J Neurosci 2002, 22:3081–3089
27. Inestrosa NC, Roberts WL, Marshall TL, Rosenberry TL: Acetylcholinesterase from bovine caudate nucleus is attached to membranes by a novel subunit distinct from those of acetylcholinesterases in other tissues. J Biol Chem 1987, 262:4441–4444
28. Laemmli UK: Cleavage of structural proteins during the assembly of the head of bacteriophage T4. Nature 1970, 227:680–685
29. Ellman GK, Courtney KD, Andress V, Featherstone RM: A new rapid colorimetric determination of acetylcholinesterase activity. Biochem Pharmacol 1961, 1:88–95
30. Klunk WE, Pettegrew JW, Abraham DJ: Quantitative evaluation of Congo red binding to amyloid-like proteins with a β-pleated sheet conformation. J Histochem Cytochem 1989, 37:1273–1281
31. Schagger H, von Jagow G: Tricine-sodium dodecyl sulfate-polyacrylamide gel electrophoresis for the separation of proteins in the range from 1 to 100 kDa. Anal Biochem 1987, 166:368–379
32. Paxinos G, Watson C: The Rat Brain in Stereotaxic Coordinates, ed 2. New York, Academic Press, 1986
33. Côté SL, Ribeiro-Da-Silva A, Cuello AC: Immunocytochemistry II. Edited by AC Cuello. New York, John Wiley & Sons, 1993
34. Elghetany MT, Saleem A: Methods for staining amyloid in tissues: a review. Stain Technol 1988, 63:201–212
35. Puchtler H, Sweat F, Levine M: On the binding of Congo red by amyloid. J Histochem Cytochem 1961, 10:355–364
36. Dickson DW, Farlo J, Davies P, Crystal H, Fuld P, Yen SH: Alzheimer's disease. A double-labeling immunohistochemical study of senile plaques. Am J Pathol 1988, 132:86–101
37. Dickson DW: The pathogenesis of senile plaques. J Neuropathol Exp Neurol 1997, 56:321–339
38. Glenner GG, Deanes ED, Page DL: The relation of the properties of Congo red-stained amyloid fibrils to the conformation. J Histochem Cytochem 1972, 20:821–826
39. Snow AD, Sekiguchi R, Nochlin D, Fraser P, Kimata K, Mizutani A, Arai M, Schreier WA, Morgan DG: An important role of heparan sulfate proteoglycan (Perlecan) in a model system for the deposition and persistence of fibrillar A β-amyloid in rat brain. Neuron 1994, 12:219–234
40. Luckenbill-Edds L: Laminin and the mechanism of neuronal outgrowth. Brain Res Brain Res Rev 1997, 23:1–27
41. Murtomaki S, Risteli J, Risteli L, Koivisto UM, Johansson S, Liesi P: Laminin and its neurite outgrowth-promoting domain in the brain in Alzheimer's disease and Down's syndrome patients. J Neurosci Res 1992, 32:261–273
42. Morgan C, Garrido J: Laminin dissaggregates amyloid β-fibrils. Neurobiol Aging 1998, 19:S45
43. Morgan C, Inestrosa NC: Interactions of laminin with the amyloid β peptide. Implications for Alzheimer's disease. Braz J Med Biol Res 2001, 34:597–601
44. Morgan C, Bugueño MP, Garrido J, Inestrosa NC: Laminin affects polymerization, depolymerization and neurotoxicity of amyloid-β peptide. Peptides 2002, 23:1229–1240
45. Pike CJ, Cummings BJ, Cotman CW: Early association of reactive astrocytes with senile plaques in Alzheimer's disease. Exp Neurol 1995, 132:172–179
46. Sigurdsson EM, Lee JM, Dong XW, Hejna MJ, Lorens SA: Bilateral injections of amyloid-β 25-35 into the amygdala of young Fischer rats: behavioral, neurochemical, time dependent histopathological effects. Neurobiol Aging 1997, 18:591–608
47. Soto C, Brañes MC, Alvarez J, Inestrosa NC: Structural determinants of the Alzheimer's amyloid β-peptide. J Neurochem 1994, 63: 1191–1198
48. Bronfman FC, Garrido J, Alvarez A, Morgan C, Inestrosa NC: Laminin inhibits amyloid-β-peptide fibrillation. Neurosci Lett 1996, 218: 201–203
49. Bronfman FC, Alvarez A, Morgan C, Inestrosa NC: Laminin blocks the assembly of wild-type Aβ and the Dutch variant peptide into Alzheimer's fibrils. Amyloid 1998, 5:16–23

50. Monji A, Tashiro K, Yoshida I, Hayashi Y, Tashiro N: Laminin inhibits Aβ 40 fibril formation promoted by apolipoprotein E4 in vitro. Brain Res 1998, 796:171–175
51. Frautschy SA, Baird A, Cole GM: Effects of Alzheimer β-amyloid cores in rat brain. Proc Natl Acad Sci USA 1991, 88:8362–8366
52. Inestrosa NC, Reyes AE: Acetylcholinesterase induces amyloid formation and increases neurotoxicity of Alzheimer's fibrils. Neurobiol Aging 1998, 19:S44
53. Reyes AE: Characterization of New Animal Models for the Study of Alzheimer's Disease. Ph.D. thesis. Pontifical Catholic University of Chile, 2000
54. Chacón MA, Reyes AE, Inestrosa NC: Acetylcholinesterase induces neuronal cell loss, astrocyte hypertrophy and behavioral deficits in mammalian hippocampus. J Neurochem 87:195–204
55. Waite J, Cole GM, Frautschy SA, Connor DJ, Thal LJ: Solvent effects on β protein toxicity in vivo. Neurobiol Aging 1992, 13:595–599
56. Abe E, Casamenti F, Giovannelli L, Scali C, Pepeu G: Administration of amyloid β-peptides into the medial septum of rats decreases acetylcholine release from hippocampus in vivo. Brain Res 1994, 636:162–164
57. Emre M, Geula C, Ransil BJ, Mesulam MM: The acute neurotoxicity and effects upon cholinergic axons of intracerebrally injected β-amyloid in the rat brain. Neurobiol Aging 1992, 13:553–559
58. Harkany T, Lengyel Z, Soos K, Penke B, Luiten PG, Gulya K: Cholinotoxic effects of β-amyloid (1-42) peptide on cortical projections of the rat nucleus basalis magnocellularis. Brain Res 1995, 695:71–75
59. Rees T, Hammond PI, Soreq H, Younkin S, Brimijoin S: Acetylcholinesterase promotes β-amyloid plaques in cerebral cortex. Neurobiol Aging 2003, 24:777–787